International Journal of Biological Macromolecules 96 (2017) 111–117

Contents lists available at ScienceDirect

International Journal of Biological Macromolecules

journal homepage: www.elsevier.com/locate/ijbiomac

Molecular mechanism of lysozyme adsorption onto chemically modified alginate guar gum matrix

Ma. Emilia Brassesco, Nadia Woitovich Valetti, Guillermo Picó*

Institute of Biotechnological and Chemistry Processes, CONICET and Faculty of Biochemical and Pharmaceutical Sciences, National University of Rosario, Suipacha 570, S2002RLK, Rosario, Argentina

ARTICLE INFO

Article history:
Received 31 May 2016
Received in revised form 17 October 2016
Accepted 12 December 2016
Available online 13 December 2016

Keywords:
Alginate
Guar gum
Polyelectrolytes
Lysozyme
Adsorption

ABSTRACT

The equilibrium isotherms and adsorption kinetics of lysozyme (LZ) on epichlorohydrin (Epi) cross-linked alginate-guar gum (Alg-GG) matrix were studied. Adsorption kinetics followed a pseudo-first-order model while the equilibrium isotherm could be represented by the Freundlich equation. The maximal amount of LZ adsorbed onto this matrix was around 2.4 mg per g of hydrated matrix at pH 7.00. The adsorption mechanism was associated to a simple diffusion process with a weak columbic interaction between LZ and the matrix. The presence of NaCl 0.3 M induced a total displacement of the LZ from the matrix. Under this condition, the percentage of desorbed protein was 95%. Successive cycles of adsorption-washing-elution were performed and the results showed the reversibility of the process and the usefulness of the method for enzyme purification and separation. A last successful step was carried out for the purification of LZ from egg white as natural source. The model proved to be useful applied as a platform design in the isolation and purification of proteins.

1. Introduction

One important tool in scaled up protein bioseparation is adsorption. This technique makes use of the adsorption capacity of a solid phase to bind molecules present in a solution. The target molecules would separate from their natural sources which are very complex systems composed of a great number of different macromolecules (proteins, nucleic acid), membranes, cells, etc. The highest cost in industrial enzyme production is the process of isolation, concentration and purification; therefore, it is necessary to design new non-expensive and environmentally-friendly methods to be applied in scaling up. In the last years, adsorption processes have been widely developed for use in the insolation of macromolecules at scaling up level. However, commercial adsorption matrixes are expensive and have short shelf life [1]. As a result, it is desirable to design new cost-efficient systems with high adsorption capacity.

Polyelectrolytes, such as alginate (Alg; COOH), carrageenan (SO_3H) and chitosan (NH_3), have been used to obtain non-soluble matrixes with high capacity to adsorb proteins due to the presence of electrically charged groups, and their capacity to become non-soluble under certain experimental condition and act as ionic exchangers [2–4]. The advantages of using these matrixes are that they are easy to prepare and dispose of into the environment with no negative impact as well as being cost-efficient. Negatively or positively charged polyelectrolyte matrixes have been used for enzyme immobilization, delivery of drugs, etc. [5–7]. In addition, the high adsorption capacity of small molecules, such as, heavy metals and aromatic contaminants in water, in polyelectrolyte non-soluble matrixes have been reported in previous works [8,9]. However, there are few reports on enzyme adsorption capacity onto these matrixes, especially about the potential application of these systems in the scale up of protein isolation. Rodriguez et al.[10] studied the adsorption of cellulase in batch and column using a mixture of two polyelectrolytes of opposite electrical charge –chitosan and Alg- and reported an enzymatic recovery of 29%. This low yield can be due to a decrease in the number of positive charges of chitosan through the interaction with Alg negative charges. Godin et al.[11] recovered human IgG using a matrix of dye-epoxide ligand Chitosan/Alg. However, at present there are not many studies on the molecular mechanism of adsorption of proteins onto Alg matrixes, including the analysis of the adsorption kinetics and their respective isotherms, the determination of thermodynamic parameters, and a correlation between these results and those obtained using dynamic adsorption (in bed) that should

Abbreviations: GG, guar gum; Alg, alginate; LZ, lysozyme; Epi, epichlorohydrin.

* Corresponding author at. Facultad de Ciencias Bioquímicas y Farmacéuticas, Universidad Nacional de Rosario, Suipacha 570, S2002RLK, Rosario, Argentina.
E-mail address: gpico@fbioyf.unr.edu.ar (G. Picó).

http://dx.doi.org/10.1016/j.ijbiomac.2016.12.029
0141-8130/

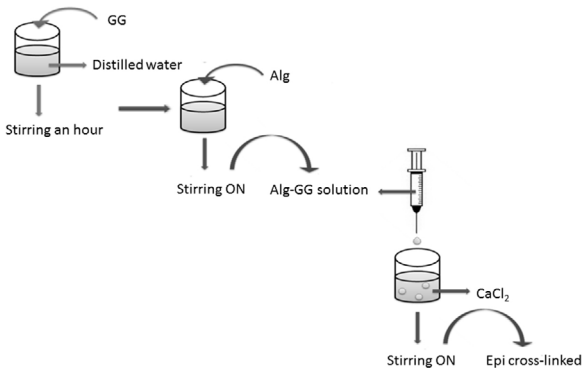

Fig. 1. Schematic representation of non-soluble Alg-GG beads preparation.

give very useful information to apply these matrixes in the bioseparation of enzymes.

In this work the molecular mechanism of LZ adsorption onto a negatively charged matrix formed by Alg and GG cross-linked with Epi was analyzed, with the goal of applying this system to the isolation and purification process of industrial enzymes.

2. Materials and methods

2.1. Chemical

Alginic acid sodium salt (Alg), guar gum (GG), epichlorohydrin (Epi) and lysozyme from chicken egg (LZ) were purchased from Sigma-Aldrich and used without further purification. All other reagents were also of analytical grade. The solutions were prepared with distilled water.

2.2. Preparation of non-soluble Alg-GG beads (adsorbent)

25 mg of GG were dissolved in 25 mL of distilled water. Alg was dissolved in the GG solution and stirred until complete dissolution. Distinct Alg-GG weight ratios were prepared: 0.6%:0.5% and 1.0%:0.5%. Beads were formed by dropping this solution through a syringe into a 50 mL of 0.1 M $CaCl_2$ solution according to the methods previously reported [11,12]. The beads were kept stirring overnight. Cross-linked Alg-GG particles were prepared by adapting the procedure of Roy et al. [12]. Fig. 1 shows the schematic representation of non-soluble Alg-GG beads preparation. Alg-GG beads (5 g) were transferred to absolute ethanol containing 0.1 M $CaCl_2$ (25 mL) and incubated for 30 min at 45 °C. Two different Epi volumes (1.5 mL and 3 mL) were added in small aliquots to this solution and were constantly stirring for 10 min. Then, two different 5N NaOH volumes (3.2 mL and 6.4 mL) were added to such solution and kept overnight at 30 °C. Finally, acetic acid was added to the system until the pH became neutral. The matrix was washed with a 3:1 mixture (v/v) of absolute ethanol and water, with 95% ethanol three times and finally, with distilled water several times. The matrix was finally re-suspended in distilled water.

2.3. Characterization of the adsorbents

2.3.1. Fourier transform infrared (FTIR) spectroscopy

Infrared transmission spectra were obtained using a Perkin-Elmer Spectrum One Model Spectrometer. The liophilized sample was mixed with dry KBr and then, ground to a fine powder using an agate mortar and compressed in a hydraulic press at a pressure of 10,000 psi to obtain KBr disks. Each KBr disk was scanned 3 times over wavenumber range of 400–4000 cm^{-1}, at room temperature. The lyophilisation process of frozen gels at −50 °C was previously carried out to form porous scaffolds.

2.3.2. pH_{ZPC} of the adsorbent

The pH at zero-charge point (pH_{zpc}) of the adsorbent was estimated by pH measurements before and after contact with the solid. In assays, 0.5 g of the adsorbent was placed in 20 mL of solution of KCl 20 mM, with a pH ranging from 2.0 to 8.0. The medium pH was adjusted with HCl (0.1 mol/L) or NaOH (0.1 mol/L). The solutions were stirred for 24 hs and then the pH was measured. The ($pH_{final}-pH_{initial}$) versus $pH_{initial}$ graph was plotted, and the pH_{zpc} value was estimated from this graph [13].

2.4. Protein estimation

The concentration of protein in the medium was evaluated at 280 nm using a UV–vis spectrophotometer. A calibration curve was performed using dilutions of a standard LZ solution of 10 mg/mL.

2.5. Batch adsorption experiments

All adsorption experiments were conducted in batch mode for an hour at a stirring rate of 30 rpm.

2.5.1. Determination of the best adsorption system

For the adsorption of commercial LZ, different systems were prepared by varying many conditions such as LZ initial concentration (0.0498 mg/mL, 0.099 mg/mL, and 0.1639 mg/mL), working medium pH (6.0, 7.0 and 8.0), ionic strength (0 and 150 mM NaCl), the Epi volume added to the system to induce cross-linking (1.5 and 3.0 mL) and the total concentration of Alg in order to obtain the matrix (0.6 and 1.0% p/V). In all the cases, 3 mL of a different concentration of LZ in 20 mM phosphate buffer was incubated with 100 mg of hydrated cross-linked Alg-GG matrix. The mixtures were stirred until the adsorption equilibrium was reached and the free protein in the supernatant was determined. The amount of LZ adsorbed was calculated from mass balance. The data were processed as percentage of protein adsorbed per g of matrix or as mass of adsorbed LZ over mass unit of hydrated matrix. All the measurements were carried out at 25 °C.

2.5.2. Adsorption kinetics

Experiments of batch kinetics adsorption of commercial LZ onto cross-linked Alg-GG beads were carried out by measuring the concentration of free LZ in the supernatant over time. To analyse the adsorption kinetic mechanism, the adsorbed LZ amounts over mass unit of matrix vs. time were fitted with two models: pseudo-first and pseudo-second order. The kinetic adsorption was assayed at two temperatures (6 °C and 25 °C), at two pH values (6.0 and 8.0), and at three different initial concentrations of enzyme (0.05, 0.1, and 0.16 mg/mL). The mixtures were prepared with 20 mM phosphate buffer and were constantly stirred at 30 rpm until the adsorption equilibrium was reached.

2.5.3. Adsorption isotherms

Adsorption isotherm of LZ was determined by equilibrating different concentrations of LZ with 100 mg cross-linked Alg-GG beads at pH 6.0 and 8.0 and two different temperatures: 25 °C and 6 °C. The mixtures were stirred until the adsorption equilibrium was reached and the free protein in the supernatant was determined. The amount of LZ adsorbed at equilibrium time by unit of adsorbent mass (m) was calculated by the following equation:

$$Q_{eq} = \frac{Vx\left(C_{eq} - C_0\right)}{m} \quad (1)$$

where Q_{eq} is the quantity of protein adsorbed per gram of adsorbent (mg/g), C_0 is the protein initial concentration in solution (mg/mL) and C_{eq} is the protein residual concentration in the supernatant at equilibrium (mg/mL), V is the volume of solution (mL) and m is the mass of adsorbent (g). The results were expressed as Q_{eq} vs. C_{eq}.

In order to estimate the validity of isotherm models with experimental data, the Langmuir, Freundlich and Hill models were tested [14,15].

2.6. Thermodynamic evaluation

The thermodynamic state functions (free energy, enthalpy and entropy) are important indicators when estimating the mechanism of the adsorption process. A distribution coefficient K_D reflects the binding ability of the surface for a molecule. The K_D is defined as follows:

$$K_D = \frac{C_s}{C_{eq}} \quad (2)$$

where C_s is the amount of LZ adsorbed in the solid matrix (mg/g) and C_{eq} is the amount of free LZ in solution in equilibrium with the adsorbed LZ (mg/mL). K_D can be obtained from extrapolating C_{eq} to zero in the plots of ln (C_s/C_{eq}) vs C_{eq} at both temperatures [16]. The standard Gibbs energy (ΔG°) was estimated by applying the thermodynamic equation as follows:

$$\Delta G^\circ = -RTlnK_D \quad (3)$$

where R is the universal gas constant (1.98 cal/molK), T is the absolute temperature (K) and K_D is the distribution coefficient of the enzyme between the adsorbed layer and the solution. The enthalpic change (ΔH°) was calculated by applying the van't Hoff equation:

$$ln\frac{K_{D,298}}{K_{D,279}} = \frac{\Delta H^\circ}{R}\left(\frac{1}{279} - \frac{1}{298}\right) \quad (4)$$

and the entropic change (ΔS°) from the well-known equation:

$$\Delta G^\circ = \Delta H^\circ - T\Delta S^\circ \quad (5)$$

2.7. Protein release from the matrix

LZ elution from the matrix was carried out at 25 °C. After adsorption, the matrix loaded with the enzyme was washed with the working buffer until a negligible 280 nm absorbance measurement. For desorption, the beads were suspended in different media and stirred for 1 h. Finally, the concentration of LZ in the supernatant was measured. The conditions assayed were: 20 mM phosphate buffer, pH 7.0 with 0, 150, 300 and 500 mM NaCl. First, data were expressed as percentage of released protein under the different conditions. Besides, desorption kinetics was measured under the best conditions determined above. The measurements were carried out at 25 °C.

2.8. Recycling capacity of the matrix

In order to study the reutilization of the matrix, successive cycles of adsorption-washing-desorption were carried out by using the same matrix as adsorbent and an excess of protein. The concentration of recovered LZ was determined at each step. The data were expressed as percentage of released protein in each cycle. The measurements were carried out at 25 °C.

2.9. Data analysis

A non-linear regression analysis was applied to estimate the isothermal and kinetic model parameters. A non-linear regression was performed using a trial and error method with the help of Sigma Plot v12 software. In the trial and error procedure, isothermal and kinetic parameters were estimated by maximizing the coefficient of determination R^2 (sum of squares) and minimizing the value of SS (least sum of squares). Both coefficients have been widely employed to measure the fitting degree of the isothermal and kinetic model to adsorption data [17]. The coefficients were calculated according to the following equations:

Error sum of squares:

$$SS = \Sigma_i^p \left(q_{eq,cal} - q_{eq,mean}\right)^2 \quad (6)$$

R^2 coefficient:

$$r^2 = \left(\frac{\left(q_{e,meas} - q_{e,calc}\right)^2}{\sum\left(q_{e,meas} - \bar{q}_{e,calc}\right)^2 + \left(q_{e,meas} - q_{e,calc}\right)^2}\right)$$

where $q_{(eq,cal)}$ and $q_{(eq,means)}$ are the equilibrium capacity obtained from the models and the equilibrium capacity from the experimental data, respectively.

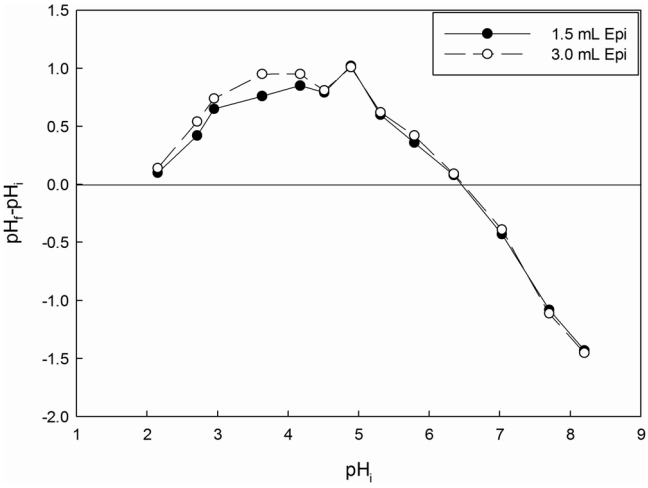

Fig. 2. pH_{zpc} of the adsorbent (0.6:0.5 ratio Alg-GG beads treated with different Epi volume). Temperature: 25 °C.

2.10. Evaluation of LZ purification from a natural source

To study the purification of LZ from a natural source, we selected eggs obtained from a nearby farm and carried out a pre-treatment which consisted in the separation of the white from the yolk. The white was diluted four times with 20 mM phosphate buffer pH 7.0. The solution pH was adjusted with HCl (cc). Finally, the solution was centrifuged at 10,000 rpm during 10 min at 4 °C. A cycle of adsorption-washing-desorption was then carried out in the best conditions obtained above and aliquots of every step were analyzed by sodium dodecyl sulphate polyacrylamide gel electrophoresis (SDS-PAGE) using a vertical system. The running time was about 120 min and the constant intensity was 25 mA for the resolving gel. Proteins were stained with Coomassie brilliant blue.

3. Results

3.1. Physicochemical characterization of the matrix

Fig. 2 shows a pH_{zpc} value of 6.4 obtained for 0.6%:0.5% ratio of Alg-GG matrixes with both Epi volumes (1.5 mL and 3.0 mL). Below the pH_{zpc} value, the solid material has a positive surface charge, promoting the adsorption of anions, and whereas the pH_{zpc} value the surface is negatively charged, favoring adsorption of cations [13].

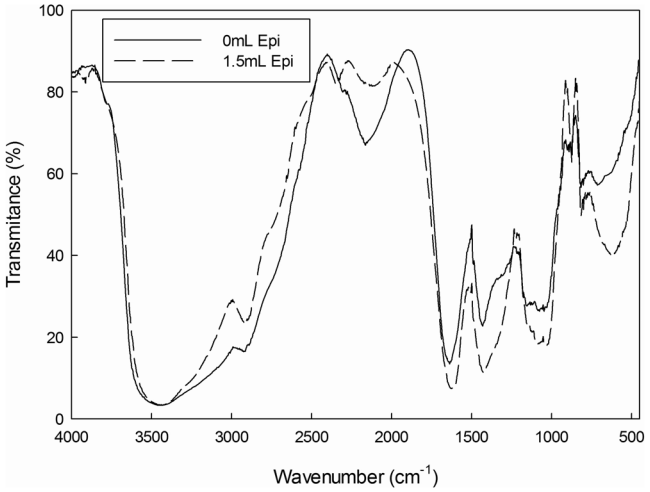

Fig. 3. IR spectrum of the Alg-GG matrixes (0.6:0.5 ratio) without and with cross-linked Epi.

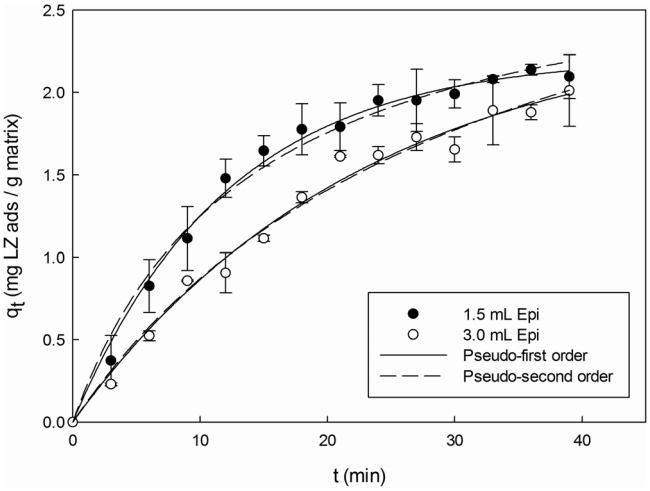

Fig. 4. Kinetic of LZ adsorption onto Alg-GG matrixes. Medium: 20 mM phosphate buffer pH 7.0. Initial LZ concentration: 0.16 mg/mL. Temperature: 25 °C.

Table 1
Percentage of LZ adsorbed for each of the systems tested.Medium: 20 mM phosphate buffer pH 7.0.Initial LZ concentration: 0.16 mg/mL. Temperature: 25 °C.

System	Epi (mL/5 g of system)	Alginate initial concentration (% p/v)	pH	% of LZ adsorbed
1	1.5	0.6	6	13.00 ± 0.08
2	3.0	0.6	6	56 ± 2
3	1.5	0.6	7	80 ± 2
4	3.0	0.6	7	77 ± 2
5	1.5	0.6	8	28.6 ± 0.4
6	3.0	0.6	8	24.7 ± 0.3
7	1.5	1.0	6	74 ± 2
8	3.0	1.0	6	26 ± 3
9	1.5	1.0	7	62 ± 1
10	3.0	1.0	7	83 ± 3
11	1.5	1.0	8	26 ± 3
12	3.0	1.0	8	57 ± 14

The FTIR spectrum of Alg-GG and cross-linked Alg-GG beads are shown in Fig. 3. The peak that mostly characterizes epoxide groups –the one that is associated to axial deformation of C—O—C observed at 1120 cm^{-1}- has high intensity for cross-linked beads when compared to the untreated control. The bands around 1030 cm^{-1} (C—O—C stretching) are attributed to the polysaccharide structure. In addition, the bands at 1617 and 1417 cm^{-1} are assigned to asymmetric and symmetric stretching peaks of Alg carboxyl groups. The peak at 3000 cm^{-1} corresponds to the hydroxyl groups of GG and Alg polysaccharides [10,12]. These results confirm the success of the cross-linking reaction.

3.2. Optimization of LZ adsorption by cross-linked Alg-GG beads

In order to determine the matrix composition that has the best adsorption capacity, many systems were designed in which the following variables were considered: pH, total Epi concentration and Alg-GG ratio whereas the dependent variable was the percentage of LZ adsorbed per unit of matrix mass. The results are shown in Table 1.

The best system for the adsorption of LZ was system 10. However, systems 3 and 4 showed a high percentage of LZ adsorbed and have the advantage of using a lower initial concentration of Alg. As a consequence, the rest of the measurements in this work were made with the same conditions as systems 3 and 4.

3.3. Kinetic studies

The kinetics of adsorption was assayed at two temperatures and three different initial amounts of LZ. Fig. 4 shows the experimental data obtained at 25 °C, constant initial LZ concentration and two different Epi volumes for the cross-linking step. It can be seen that, in both cases, the adsorbed protein increases with contact time until it reaches a plateau. The point where the plateau begins is the equilibrium time required to achieve the maximum adsorption under these conditions. Also, it can be seen that the major amount of Epi induced a decrease in LZ adsorption.

To analyse the adsorption kinetics mechanism, the experimental data at different temperatures and initial concentrations of LZ were fitted with two models called, pseudo-first-order and pseudo-second-order [18,19] respectively, as shown in Eqs. (8) and (9).

$$q_t = q_e\,(1 - e^{-k_1 t}) \tag{8}$$

$$q_t = \frac{k_2 q_e^2 t}{1 + k_2 q_e t} \tag{9}$$

where k_1 and k_2 are the first and second order kinetics constant, respectively, and q_t and q_e are the amounts of LZ adsorbed per g of matrix in a time "t" and at the equilibrium, respectively. Table 2 shows the parameters of the kinetic models and the regression correlation coefficients (R^2). It can be seen that SS values obtained from fitting to pseudo first order kinetics are low and the correlation coefficient values were found to be greater than 0.99, which shows the applicability of the pseudo first order as model of LZ adsorption. Besides, q_t values obtained for the first order are in concordance with the visual value shown in Fig. 4.

The activation energy of the adsorption process was calculated using the Arrhenius equation:

$$ln\frac{k_{279K}}{k_{298K}} = \frac{E_a}{R}\left(\frac{1}{T^{298K}} - \frac{1}{T^{279K}}\right) \tag{10}$$

where R is the universal gas constant ($1.9817.10^{-3}$ kcal/mol.K), T is the absolute temperature (K) and E_a is the adsorption activation energy (kcal/mol).The magnitude of E_a may give an idea of the type of adsorption. The obtained values of E_a were 4.34 and 7.3 kcal/mol for cross-linked system with 1.5 and 3.0 ml of Epi, respectively. These values are low and it can thus be concluded that the process is controlled by interactions of physical nature [17].

The solute transfer is usually characterized by external mass transfer (boundary layer diffusion), intra-particle diffusion or both.

Table 2
Kinetic parameters for the adsorption of LZ onto Alg-GG matrixes cross-linked with two different Epi volumes (1.5 mL and 3.0 mL). Medium: 20 mM phosphate buffer, pH 7.0. Initial LZ concentration: 0.16 mg/mL. Temperature: 25 °C.

EpiVolume (mL)	Model	Q_e (mg g^{-1})	k_1 (min^{-1})	k_2 (g mg^{-1} min^{-1})	R^2	SS
1.5	Pseudo-first order	2.20 ± 0.04	(8.3 ± 0.5).10^{-2}	NA	0.9934	0.0398
	Pseudo-second order	0.4 ± 22.7	NA	(0.16 ± 3.87).10^{-4}	0.9871	0.0779
3.0	Pseudo-first order	2.40 ± 0.15	(4.4 ± 0.5).10^{-2}	NA	0.9877	0.0676
	Pseudo-second order	0.4 ± 6.4	NA	(7.5 ± 0.08).10^{-2}	0.9861	0.0759

Table 3
Relative diffusion coefficient (K_{id}) calculated from Eq. (11). Medium: 20 mM phosphate buffer pH 7.0.Initial LZ concentration: 0.16 mg/mL. Temperature: 25 °C.

EpiVolume (mL)	K_{id} (g mg^1 min^{-1})				
	Li^+	Control	K^+	Rb^+	Cs^+
1.5	0.38 ± 0.04	0.37 ± 0.02	0.09 ± 0.04	0.08 ± 0.04	0.01 ± 0.04
3.0	0.52 ± 0.02	0.36 ± 0.02	0.13 ± 0.02	0.10 ± 0.01	≅0

The adsorption dynamics can be described by the following three consecutive steps [19]:

- Transport of the solute from the bulk solution through the liquid film to the adsorbent surface;
- Solute diffusion into the pore of the adsorbent except for a small quantity of sorption on the external surface. Parallel to this there is intra-particle transport mechanism of the surface diffusion;
- Adsorption of solute on the interior surfaces of the pores and capillary spaces of the adsorbent. The last step is assumed to be rapid and considered to be negligible.

The overall rate of adsorption will be controlled by the slowest step, which would be either film diffusion or pore diffusion. The most commonly used technique for identifying the mechanism involved in the adsorption processes is to fit the experimental data in an intra-particle diffusion plot. Previous studies by various researchers [18,19] showed that the plot of q_t versus $t^{0.5}$ represents multilinearity, which characterizes the steps involved in a adsorption process. The intra-particle diffusion model is given in a simplified form by Dogan et al. [17]:

$$q_t = K_{id} t^{0.5} + C \quad (11)$$

where K_{id} is the intra-particle diffusion coefficient (mg g^{-1} min$^{-0.5}$) and C is a constant related to the extent of the boundary layer effect. Thus, the K_{id} (mg g^{-1} min$^{-0.5}$) value can be obtained from the slope of the plot q_t (mg g^{-1}) versus $t^{0.5}$ (min$^{0.5}$). A linear relationship between q_t and $t^{0.5}$ was found, and the slope of the strength line (K_{id}) remained a constant value (data not shown). This effect was observed for the two Epi relations assayed, suggesting that the diffusion coefficient does not depend on the matrix cross-linking grade. As intra-particle diffusion remained constant, adsorption is driven only by the boundary layer, which is represented by the intersection of the plot with the y axes (zero time) (C), which reflects the solute initial concentration on the boundary layer. As C values were not dependent on the initial LZ concentration, it can be confirmed that solute diffusion through the layer is the only driving force of adsorption kinetics [20].

This finding can be due to the small size of the LZ molecules which can diffuse into the matrix pore. The low E_a observed is in agreement with the presence of a simple solute diffusion process. The protein kinetics diffusion was also assayed in the presence of different cations of the Hofmeister series as chloride form.

Table 3 shows the effect of the cations on K_{id} values. A linear relationship was found according to Eq. (11) in presence of the cations assayed (data not shown). As shown Table 3, the diffusion coefficient (K_{id}) is slightly increased in the presence of Li^+, while the other cations induced a significant decrease as follows: $K^+ > Rb^+ > Cs^+$. This effect cannot be attributed to an electrostatic effect because the ionic strength of the medium was constant. Since the matrix is formed by polysaccharides, the number of water molecules ordered in the environment of the polysaccharide chains is high and their presence is fundamental for the LZ diffusion across the pores of the matrix to interact with the COO^- of Alg. The C value remained constant for all the cases, (data not shown), as this parameter is related to the extent of the boundary layer, it can be concluded that the Hofmeister series does not modify it. Thus, the water layer of hydration on the matrix surface and in the pore wall is not modified. Each alginate saccharine unit has the capacity to bind 11–12 water molecules [21]. The effect of alginate on the dynamics of water is restricted only to the first hydration shell, which the extension of this barrier is great due to the high matrix porosity. Hence, this water layer is a barrier which should be overcome by the molecule of LZ as a previous process to interact with alginate COO^- monomer. Lutter et al. [22] suggested that hydration of cations plays a key role in determining the interactions between the cations and a polymer. Larger monovalent cations such as: Rb^+ and Cs^+ have weaker interactions with water molecules through electrostatic attraction which induces salting-in effects on the polymer as compared to smaller monovalent cations (Li^+) [22,23].

It has been demonstrated that the electrophoretic mobility of an electrically charged particle is influence by the Hofmeister series of cations [24], based on the an interaction between the surfaces negative electrical charge and the mobile particles with opposite electrical charge, such is the case of a protein. Our finding showed that cations of the Hofmeister series modified the diffusion coefficient as follows: $Cs^+ < Rb^+ < K^+ < Li^+$. This trend in the mobility reflects the affinity of the different cations to the negatively charged electrical surface of the Alg-GG matrix. Therefore, poorly hydrated cations such as Cs^+ interact more strongly with the charged electrical surface of Alg-GG and, hence, will reduce the magnitude of the charged surface and therefore the LZ diffusion to the surface of the matrix. The strongly hydrated Li^+ ion interacts weakly on the Alg-GG surface and wall pores, and therefore, LZ diffusion will be not modified.

3.4. Isotherm modelling

Fig. 5 illustrates the experimental equilibrium isotherm data for the Alg-GG matrix treated with 1.5 and 3.0 ml of Epi. It can be seen that the higher the concentration of Epi, the lower the adsorption capacity of the matrix, in agreement with a more closed structure of the polysaccharide chain. To optimize the design of an adsorption system for the removal of adsorbate, it is important to establish the most appropriate correlation for the equilibrium data. Various isotherm equations have been used to describe the isotherm curve [25]. For adjustment of the experimental data the following isotherm models were chosen:

i) Freundlich isotherm model: an empirical equation used for the description of multilayer adsorption with interaction between adsorbed molecules:

$$q_e = K_F C_e^{1/n_F} \quad (12)$$

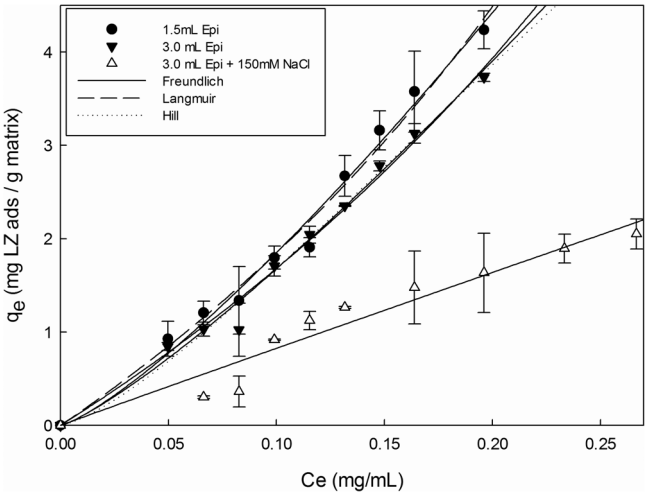

Fig. 5. Adsorption isotherm of LZ onto non-soluble Alg-GG beads. Medium: 20 mM phosphate buffer, pH 7.0.Temperature: 25 °C.

where C_{eq} indicates the equilibrium concentration of adsorbate and K_F and n_F are the Freundlich constants characteristic of the system. K_F and n_F are indicators of adsorption capacity and adsorption intensity, respectively [25].

ii) Langmuir isotherm model: This model describes the formation of a monolayer adsorbate on the surface of the adsorbent without interactions between adsorbed molecules:

$$q_e = \frac{Q_0 K_L C_e}{1 + K_L C_e} \quad (13)$$

where Q and C_{eq} are the amount of protein adsorbed per weight unit of biomass and the unabsorbed protein concentration in solution at equilibrium, respectively. Q_{max} is the maximum amount of protein absorbed per weight unit of adsorbent to form a complete monolayer and K_L is the Langmuir adsorption constant related to the affinity of the binding sites [14].

iii) Hill isotherm: The Hill isotherm model has been applied to systems which present non-ideal competitive adsorption, to explain the binding of a molecule onto homogeneous substrate. The model assumes that the adsorption process as a cooperative phenomenon, with the ligand binding ability at one site on the matrix, may influence the binding capacity of other sites:

$$q_e = \frac{Q_0 {C_e}^{n_H}}{K_H + {C_e}^{n_H}} \quad (14)$$

Where q_e (mg/g matrix) is the amount of adsorbed protein at the equilibrium; Q_0 (mg/g matrix) is the maximal capacity of adsorption of the matrix, C_e is the free (unbound) Chy concentration, K_H is the Hill constant and *nH* is the Hill cooperativity coefficient of the binding interaction [25].

The statistical analysis of error function shows that both systems data fit to Freundlich model (see Table 4) at the two temperatures assayed (data not shown). The Freundlich model is in agreement with the low activation energy found associated to the adsorption process. The K_F value decreased with an increase in the polysaccharide chain cross-linking by Epi action, as shown in Table 4. The Langmuir and Hill models yielded anomalous parameters demonstrating that the Freundlich model is the correct one to fit the experimental data.

Table 4 shows the thermodynamic variables values associated to LZ adsorption at 25 °C. The ΔH° was positive, which agrees with a physical adsorption mechanism or with a slight coulombic interaction based on the disorder of water ordered in the pores of the matrix, induced by the diffusion of LZ to them. The positive ΔS° observed agree with this mechanism. It can be seen that an increase in Epi volume at the step of cross-linking induces a decrease in both thermodynamic parameters, due to a more closed structure of the matrix treated with 3.0 mL of Epi.

3.5. Desorption conditions

The only condition of desorption assayed was the addition of NaCl to the system after the previous step of adsorption and washing of the matrix so as break the coulombic interaction. The presence NaCl 0.3 M induced a total displacement of LZ from the matrix. Under this condition, the percentage of desorbed protein was 95 ± 2%.

3.6. Regeneration study

Any adsorbent is economically viable as long as it can be regenerated and reused in many cycles of operation. First, six cycles were carried out over twenty days. In all the cycles the mean LZ adsorption was around 50% of the total protein present, but desorption with NaCl 0.3 M was almost 100%. It can be seen that the adsorption capacity of the matrix was not modified and the enzyme recovery is total in this short period during the recycling test.

3.7. Purification of LZ starting egg white

A cycle of adsorption-washing-desorption was carried out for the purification of LZ of egg white applying the best conditions obtained above. The aliquots of each step were separated and then analyzed by SDS-PAGE. Fig. 6 shows the purification of LZ. The lane corresponding to desorption step (fourth lane) shows the predominant band corresponding to LZ with a minor quantity of contaminant proteins in contrast to the second and third lane which represented the egg white homogenate and the adsorption step respectively.

Table 4
Isotherm parameters and thermodynamic constant of LZ adsorption onto Alg-GG matrix. Temperature: 25 °C.

Model	Epi Volume (mL)	K_F	K_L	K_H	$1/n_F$	Q_0 (mg.g^{-1})	n_H	R^2	SS
Freundlich	1.5	33.5 ± 4.6	N.A	N.A	1.3 ± 0.07	N.A	N.A	0.9878	0.1895
	3.0	27.7 ± 3,5	N.A	N.A	1.2 ± 0.07	N.A	N.A	0.9891	0.1318
Langmuir	1.5	N.A	−1.5 ± 0.3	N.A	N.A	−10.5 ± 3.4	N.A	0.9875	0.1939
	3.0	N.A	−1.3 ± 0.3	N.A	N.A	−11.6 ± 3.0	N.A	0.9875	0.1521
Hill	1.5	N.A	N.A	N.A	N.A	N.A	N.A	N.A	N.A
	3.0	0.5 ± 1.05	N.A	N.A	N.A	22.0 ± 42.2	1.4 ± 0.3	0.9895	0.1277
		ΔH (kcal mol^{-1})	ΔS (cal mol^{-1} K^{-1})						
Thermodynamics functions value	1.5	7.3	27.0						
	3.0	1.0	5.0						

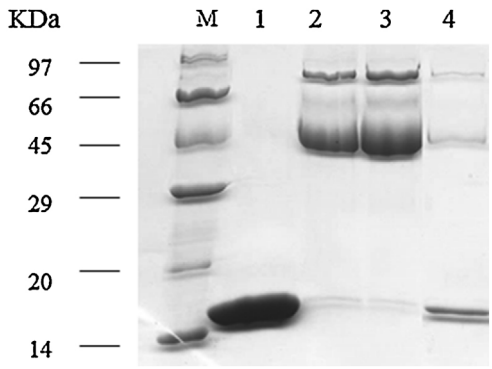

Fig. 6. SDS-PAGE (Coomassie blue staining). Sigma LZ of egg white (first lane), egg white homogenate (second lane), the adsorption step (third lane) and the desorption step (fourth lane).

4. Conclusion

Cross-linked Alg-GG beads were selected as adsorbent for the purification of LZ. The effects of pH, the cross-linking grade of the polymers and the initial protein concentration on LZ adsorption were investigated. In this paper, we proved the potential use of Alg-GG matrix as a tool for protein bioseparation and as a platform to apply this system at scaling up level, because it has an easy and inexpensive preparation. We have selected LZ, which has positive electrical charge in a wide pH range, so this protein is a good model because the results can be applied to other similar proteins such as trypsin, chymotrypsin and elastase. On the other hand, LZ has biotechnological and medical applications as well.

The optimal conditions determined were: pH 7.0, Alg initial concentration of 0.6% p/v, initial LZ concentration of 0.16 mg/mL and temperature of 25 °C. Under these conditions 2.20 mg of LZ was adsorbed per g of matrix. A previous work in our laboratory showed a maximal binding capacity of 8.0 mg Chymotrypsin (Chy) per gram of Alg-GG matrix at 8 °C [26]. A first order kinetics for the adsorption step with low activation energy was found, which suggests the participation of a physical mechanism of adsorption, such as van der Waals forces. This finding is in agreement with Freundlich isotherm model fitted the equilibrium data and with the positive ΔH° and ΔS° associated to LZ adsorption. Kinetic equations were used to analyze the adsorption kinetics at different temperatures; the kinetic data were found to be more properly explained by the pseudo first order kinetic model. The equilibrium, kinetic and thermodynamic parameters provided some basic information for the large-scale exploitation of this bio-adsorption process. The effect of the cations of the Hofmeister series on the adsorption process showed that the transfer of protein through the water boundary layer bound to the matrix surface and pore wall are driven by forces which regulate the adsorption mechanism only by diffusion.

The physical behavior of the matrix proved to be good, and to have high capacity of protein adsorption during the recycle test. It possible increase adsorption capacity using the matrix in packed bed.

Acknowledgements

This research was supported by grants from FonCyT, Projects PICT 2013 -271- Argentina Innovator 2020. We would like to thank the staff from the English Department (Facultad de Ciencias Bioquímicas y Farmacéuticas, UNR) for the language correction of the manuscript.

References

[1] V. Boeris, I. Balce, R.R. Vennapusa, M.A. Rodríguez, G. Pic&#x00F3, M.F. Lahore, Production, recovery and purification of a recombinant β-galactosidase by expanded bed anion exchange adsorption, J. Chromatogr. B 900 (2012) 32–37.
[2] P. Coimbra, P. Ferreira, H. De Sousa, P. Batista, M. Rodrigues, I. Correia, M. Gil, Preparation and chemical and biological characterization of a pectin/chitosan polyelectrolyte complex scaffold for possible bone tissue engineering applications, Int. J. Biol. Macromol. 48 (1) (2011) 112–118.
[3] D.R. Gondim, N.A. Dias, I.T. Bresolin, A.M. Baptistiolli, D.C. Azevedo, I.J. Silva Jr., Human IgG adsorption using dye-ligand epoxy chitosan/alginate as adsorbent: influence of buffer system, Adsorption 20 (8) (2014) 925–934.
[4] D. Spelzini, B. Farruggia, G. Picó, Purification of chymotrypsin from pancreas homogenate by adsorption onto non-soluble alginate beads, Process Biochem. 46 (3) (2011) 801–805.
[5] J. López-Morales, D. Sánchez-Rivera, T. Luna-Pineda, O. Perales-Pérez, F. Román-Velázquez, Entrapment of tyre crumb rubber in calcium-alginate beads for triclosan removal, Adsorpt. Sci. Technol. 31 (10) (2013) 931–942.
[6] H.A. Pawar, K. Lalitha, K. Ruckmani, Alginate beads of Captopril using galactomannan containing Senna tora gum, guar gum and locust bean gum, Int. J. Biol. Macromol. 76 (2015) 119–131.
[7] D. Tahtat, M. Mahlous, S. Benamer, A.N. Khodja, H. Oussedik-Oumehdi, F. Laraba-Djebari, Oral delivery of insulin from alginate/chitosan crosslinked by glutaraldehyde, Int. J. Biol. Macromol. 58 (2013) 160–168.
[8] A. Karagunduz, D. Unal, New method for evaluation of heavy metal binding to alginate beads using pH and conductivity data, Adsorption 12 (3) (2006) 175–184.
[9] T.Y. Kim, S.Y. Cho, S.J. Kim, Adsorption equilibrium and kinetics of copper ions and phenol onto modified adsorbents, Adsorption 17 (1) (2011) 135–143.
[10] E.C. Rodrigues, B.T. Bezerra, B.V. Farias, W.S. Adriano, R.S. Vieira, D.C. Azevedo, I.J. Silva, Adsorption of cellulase isolated from aspergillus niger on chitosan/alginate particles functionalized with epichlorohydrin, Adsorpt. Sci. Technol. 31 (1) (2013) 17–34.
[11] D.R. Gondim, L.P. Lima, M.C. de Souza, I.T. Bresolin, W.S. Adriano, D.C. Azevedo, I.J. Silva, Dye ligand epoxide chitosan/alginate: a potential new stationary phase for human IgG purification, Adsorpt. Sci. Technol. 30 (8–9) (2012) 701–711.
[12] I. Roy, M. Sardar, M.N. Gupta, Cross-linked alginate–guar gum beads as fluidized bed affinity media for purification of jacalin, Biochem. Eng. J. 23 (3) (2005) 193–198.
[13] N. Fiol, I. Villaescusa, Determination of sorbent point zero charge: usefulness in sorption studies, Environ. Chem. Lett. 7 (1) (2009) 79–84.
[14] K. Foo, B. Hameed, Insights into the modeling of adsorption isotherm systems, Chem. Eng. J. 156 (1) (2010) 2–10.
[15] I. Guerrero-Coronilla, L. Morales-Barrera, E. Cristiani-Urbina, Kinetic, isotherm and thermodynamic studies of amaranth dye biosorption from aqueous solution onto water hyacinth leaves, J. Environ. Manage. 152 (2015) 99–108.
[16] A. Günay, B. Ersoy, S. Dikmen, A. Evcin, Investigation of equilibrium, kinetic, thermodynamic and mechanism of Basic Blue 16 adsorption by montmorillonitic clay, Adsorption 19 (2–4) (2013) 757–768.
[17] M. Doğan, Y. Özdemir, M. Alkan, Adsorption kinetics and mechanism of cationic methyl violet and methylene blue dyes onto sepiolite, Dyes Pigm. 75 (3) (2007) 701–713.
[18] V. Vadivelan, K.V. Kumar, Equilibrium, kinetics, mechanism, and process design for the sorption of methylene blue onto rice husk, J. Colloid Interf. Sci. 286 (1) (2005) 90–100.
[19] C. Zhou, Q. Wu, T. Lei, I.I. Negulescu, Adsorption kinetic and equilibrium studies for methylene blue dye by partially hydrolyzed polyacrylamide/cellulose nanocrystal nanocomposite hydrogels, Chem. Eng. J. 251 (2014) 17–24.
[20] E. Daneshvar, M. Kousha, M. Jokar, N. Koutahzadeh, E. Guibal, Acidic dye biosorption onto marine brown macroalgae: isotherms, kinetic and thermodynamic studies, Chem. Eng. J. 204 (2012) 225–234.
[21] K. Mazur, R. Buchner, M. Bonn, J. Hunger, Hydration of sodium alginate in aqueous solution, Macromolecules 47 (2) (2014) 771–776.
[22] J.C. Lutter, T.-y. Wu, Y. Zhang, Hydration of cations: a key to understanding of specific cation effects on aggregation behaviors of PEO-PPO-PEO triblock copolymers, J. Phys. Chem. B 117 (35) (2013) 10132–10141.
[23] Y. Zhang, P.S. Cremer, Interactions between macromolecules and ions: the Hofmeister series, Curr. Opin. Chem. Biol. 10 (6) (2006) 658–663.
[24] T. Oncsik, G. Trefalt, M. Borkovec, I. Szilagyi, Specific ion effects on particle aggregation induced by monovalent salts within the Hofmeister series, Langmuir 31 (13) (2015) 3799–3807.
[25] S. Rangabhashiyam, N. Anu, M.G. Nandagopal, N. Selvaraju, Relevance of isotherm models in biosorption of pollutants by agricultural byproducts, J. Environ. Chem. Eng. 2 (1) (2014) 398–414.
[26] N.W. Valetti, G. Picó, Adsorption isotherms, kinetics and thermodynamic studies towards understanding the interaction between cross-linked alginate-guar gum matrix and chymotrypsin, J. Chromatogr. B 1012 (2016) 204–210.